

Sub-Coulomb (d, p) stripping on the $N = 82$ isotones*

G. A. Norton, N. L. Gearhart, H. J. Hausman, and J. F. Morgan
 Department of Physics, The Ohio State University, Columbus, Ohio 43210

(Received 6 August 1973)

Stripping reactions (d, p) have been performed on ^{139}La , ^{140}Ce , ^{141}Pr , ^{142}Nd , and ^{144}Sm in which both the entrance and exit channels are below the Coulomb barrier. Reduced normalizations have been extracted from these data and are shown to be insensitive to the optical-model parameters used in the distorted-wave Born-approximation analysis. The Q dependence of the reduced normalizations is also noted.

[NUCLEAR REACTIONS ^{139}La , ^{140}Ce , ^{141}Pr , ^{142}Nd , $^{144}\text{Sm}(d, p)$ $E = 5.8$ MeV;
 measured $\sigma(\theta)$, ^{140}La , ^{141}Ce , ^{143}Nd , ^{145}Sm levels. Deduced Λ . DWBA analysis,
 $\theta = 55\text{--}165^\circ$, $\Delta\theta = 10^\circ$.]

I. INTRODUCTION

In extracting spectroscopic factors S_{ij} from (d, p) stripping data, it has been observed that S_{ij} depends strongly on the optical-model parameters used in fitting the experimental angular distribution by distorted-wave Born-approximation (DWBA) codes. In an effort to reduce the parameter dependence in S_{ij} , (d, p) reactions have been performed where both the entrance and exit channels were below the Coulomb barrier of the target nuclei. This reduces the effect of the nuclear potentials in the elastic channels. However, a strong dependence on the potential parameters used to describe the neutron bound-state well still remains.

Another quantity that can be obtained from sub-

Coulomb (d, p) stripping data is the reduced normalization Λ_{ij}^{1-3} which is essentially the normalization of the spherical Hankel function which is the transferred neutron's asymptotic wave function. Rapaport and Kerman³ have shown that Λ_{ij} is nearly independent of the geometrical parameters used to describe the neutron bound-state well for (d, p) stripping, in which both incoming and outgoing channels are below the Coulomb barrier.

We have completed an investigation of the sub-Coulomb (d, p) stripping reactions on the $N = 82$ isotones: ^{139}La , ^{140}Ce , ^{141}Pr , ^{142}Nd , and ^{144}Sm . The ground-state Q values for (d, p) stripping on these isotones were such that several low-lying states could be observed with both the deuteron and proton channels below the Coulomb barrier. The DWBA code JULIE⁴ was used to calculate re-

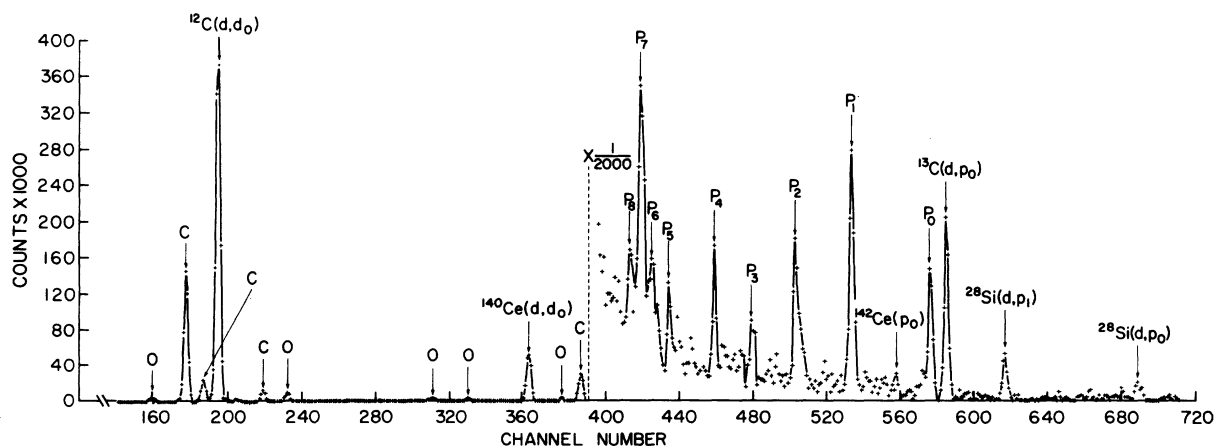


FIG. 1. The spectrum of $^{140}\text{Ce}(d, p)^{141}\text{Ce}$, taken using a deuteron beam at 5.8 MeV, for a total charge collection of $2400 \mu\text{C}$, at a detector angle of 165° . At this angle the sub-Coulomb (d, p) peaks are near their maximum yields, which is approximately 100 to 200 counts per peak. Peaks designated by O are due to reactions involving ^{16}O and those designated by C are due to reactions involving ^{12}C .

duced normalizations for a total of 16 states. The Q -value and mass-number dependence of Λ_{ij} was noted.

II. EXPERIMENTAL PROCEDURE

Carbon-backed targets of lanthanum, cerium oxide, praseodymium, neodymium oxide, and samarium were used in this experiment. All were of natural isotopic abundance, except that neodymium and samarium were enriched to 96% ^{142}Nd and 94.5% ^{144}Sm , respectively. These targets were prepared by vacuum evaporation onto 100- $\mu\text{g}/\text{cm}^2$ carbon foils. The cerium, neodymium, and samarium targets were constructed with the use of an electron gun by Micro Matter Company,⁵ while the lanthanum and praseodymium targets were constructed locally by resistance heating from a tantalum boat. The thicknesses were determined to within $\pm 10\%$ by Rutherford scattering of 2-MeV protons and were on the order of 100 $\mu\text{g}/\text{cm}^2$.

The (d, p) reactions were studied using a 5.8-MeV deuteron beam from the Ohio State University CN Van de Graaff accelerator. At this beam energy both the entrance and exit channels were below the Coulomb barrier for all states, and reasonable proton yields were still observed. The experiment was carried out in a 61-cm-diam scattering chamber⁶ using three silicon surface-barrier detectors with depletion depths sufficient to stop 12-MeV protons. A typical spectra of the $^{140}\text{Ce}(d, p)$ reaction is shown in Fig. 1.

Angular distributions were measured from 55 to 165° in 10° steps. However, since the cross sections for sub-Coulomb (d, p) fall off sharply in the

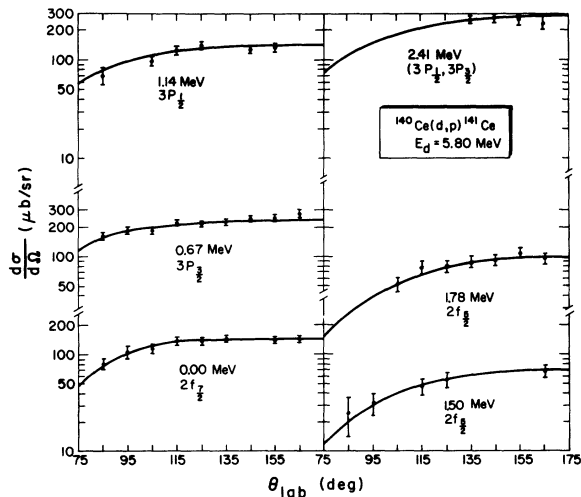


FIG. 2. Differential cross sections of the $^{140}\text{Ce}(d, p)$ reaction at $E_d = 5.8$ MeV. The solid line is the DWBA curve calculated by code JULIE.

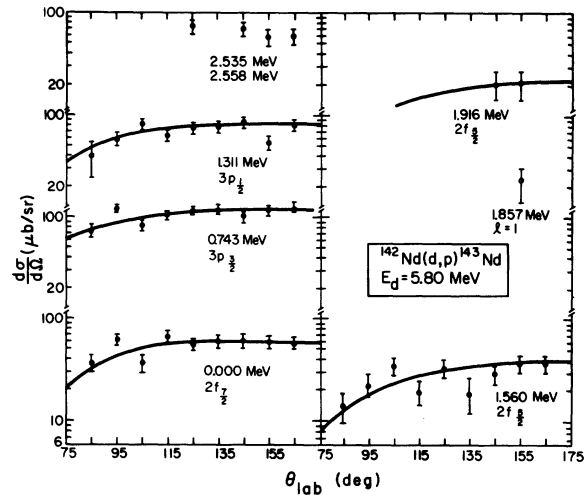


FIG. 3. Differential cross sections of the $^{142}\text{Nd}(d, p)$ reaction at $E_d = 5.8$ MeV. The solid line is the DWBA curve calculated by code JULIE.

forward angles, while the cross sections for (d, p) stripping above the Coulomb barrier tend to reach their maximum in the forward angles, the peaks of interest could not be separated from the background of light contaminants for angles from 55 through 75°. Also, (d, p) stripping on light con-

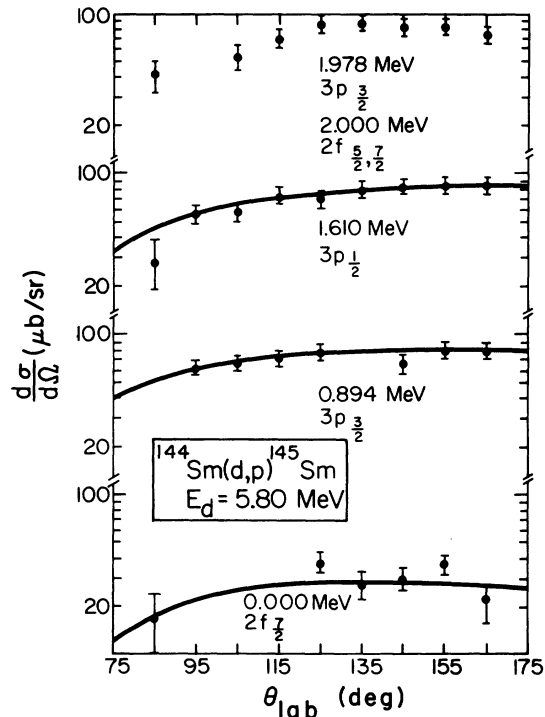


FIG. 4. Differential cross sections of the $^{144}\text{Sm}(d, p)$ reaction at $E_d = 5.8$ MeV. The solid line is the DWBA curve calculated by code JULIE.

taminants such as ^{12}C , ^{13}C , and ^{28}Si prevented the determination of the areas of some rare-earth (d, p) peaks at certain angles. The angular distributions for the sub-Coulomb (d, p) reactions on ^{140}Ce , ^{142}Nd , and ^{144}Sm are shown in Figs. 2-4. The error bars in the figures represent statistical uncertainties in the proton yields.

For the $^{139}\text{La}(d, p)$ and $^{141}\text{Pr}(d, p)$ reactions further difficulties were encountered. Both isotones have an odd proton capable of coupling to the neutron state, which causes the energy separation between states in these two isotones to be much smaller than in the even proton isotones. The last proton in ^{140}La and ^{142}Pr can be in either the $2d_{5/2}$ or the $1g_{7/2}$ state, each of which couples to the $2f_{7/2}$ neutron ground state. This leads to a multiplet of eight states for the $1g_{7/2}(p) \otimes 2f_{7/2}(n)$ coupling, and a multiplet of six states for the $2d_{5/2}(p) \otimes 2f_{7/2}(n)$ coupling. Since the resolution of the electronics used for this experiment is on the order of 50 keV full width at half maximum (FWHM), it was impossible in most cases to separate the peaks of interest. All the spin information for ^{140}La and ^{142}Pr was taken from Kern, Struble, and Sheline^{7,8}

In the ^{140}La spectra only two peaks could be separated from the background (see Fig. 5). Peak 1 contains a total of six states which range in excitation energy from 0 to 63 keV; all these states involve proton coupling to the $2f_{7/2}$ neutron ground state. Peak 2 represents only one state,

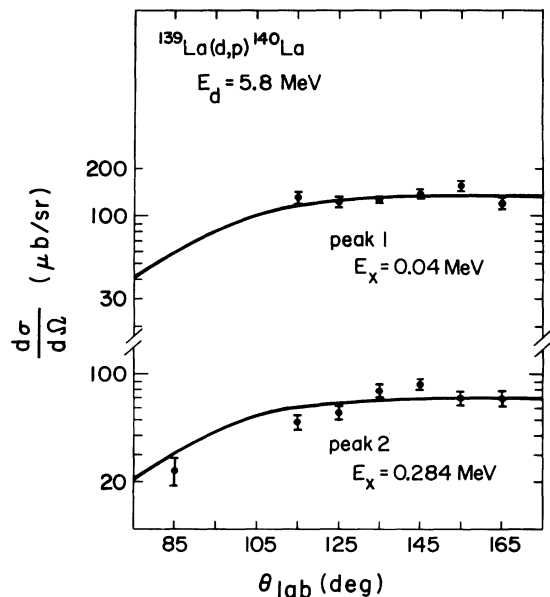


FIG. 5. Differential cross sections of the $^{139}\text{La}(d, p)$ reaction at $E_d = 5.8$ MeV. The solid line is the DWBA curve calculated by code JULIE.

the $1g_{7/2}(p) \otimes 2f_{7/2}(n)$ state with $J=7$ and excitation energy of 284 keV.

In the ^{142}Pr spectra the states were too closely packed, so that no sub-Coulomb peaks could be separated from the background contaminants.

III. ANALYSIS

The DWBA calculations used to fit the sub-Coulomb (d, p) angular distributions were carried out using code JULIE with the optical-model parameters taken from the work of Rapaport and Kerman.³ These are listed in Table I along with the form of the optical-model potential used.

The relationship between the reduced normalization and the spectroscopic factor has been explained in detail in several other articles,^{3,9,10} and will be discussed only briefly here. The equation defining Λ_{ij} is

$$\langle B|A \rangle = [(2J+1)\Lambda_{ij}]^{1/2} k^{3/2} h_{ij}^{(1)}(ikr), \quad r > R_n,$$

where

$$k = (2\mu|B_n|)^{1/2}/\hbar.$$

$\langle B|A \rangle$ is the overlap integral between the initial state of spin I and the final state of spin J , which can be thought of as the wave function of the transferred neutron, and R_n is the nuclear radius. $h_{ij}^{(1)}$ is the Hankel function of the first kind, and μ is the reduced mass of the exit channel, and B_n is the binding energy of the transferred neutron.

The equation that relates S_{ij} and Λ_{ij} is

$$k^3 \Lambda_{ij} = N_{ij}^2 S_{ij},$$

where N_{ij} is the ratio, outside the nuclear radius, of the DWBA neutron bound-state wave function to

TABLE I. Optical-model parameters for (d, p) analysis. The neutron real-well depth was varied to fit the binding energy of the transferred neutron given by $Q(d, p) + 2.224$ MeV, with $r_n^0 = 1.20$ fm and $a = 0.65$ fm. The potential used in code JULIE has the form

$$V(r) = -V(e^x + 1)^{-1} + iW \frac{d}{dx'} (e^{x'} + 1)^{-1} + V_c(r, r_{0c}),$$

where

$$x = \frac{r - r_0 A^{1/3}}{a} \quad \text{and} \quad x' = \frac{r - r_0' A^{1/3}}{a'}.$$

V_c is the Coulomb potential of a uniformly charged sphere of radius $r_{0c} A^{1/3}$.

	V (MeV)	W (MeV)	r_0 (fm)	a (fm)	r_0' (fm)	a' (fm)	r_{0c} (fm)
d	97.5	67.5	1.15	0.847	1.332	0.692	1.30
p	57.6	62	1.25	0.65	1.25	0.47	1.25

a spherical Hankel function. S_{lj} is given by

$$S_{lj} = \frac{1}{1.5} \frac{2I+1}{2J+1} \frac{\sigma_{\text{exp}}(\theta)}{\sigma_{\text{JULIE}}(\theta)}$$

The factor of 1.5 is related to the Hulthén wave function used to describe the deuteron. $\sigma_{\text{exp}}(\theta)$ is the experimentally determined differential cross section for the sub-Coulomb (d, p) reaction and $\sigma_{\text{JULIE}}(\theta)$ is the differential cross section calculated by code JULIE.

In order to test the parameter insensitivity of Λ_{lj} , several optical-model parameter variations were carried out. In the following variations, only one parameter was varied at a time, with all other parameters set to the values shown in Table I.

When the neutron-well radius r_n^0 was varied from 0.9 to 1.8 fm for the ^{141}Ce ground state (Fig. 6), the spectroscopic factor decreased by 99%, while Λ_{lj} increased by only 6%. The diffusivity of the neutron potential a_n was varied from 0.2 to 0.9 fm for the ground state of ^{141}Ce (Fig. 7). In this variation, S_{lj} decreased by 81% while Λ_{lj} decreased by less than 0.05%. Also, a spin-orbit term was added to the neutron potential and the spin-orbit potential V_{so} was varied from 0 to 3.0 MeV, producing an average change of 10% in S_{lj} ,

TABLE II. Final results.

	E_x (MeV)	n_{lj}	Λ_{lj}
^{140}La	0.04	$2f_{7/2}$	123
	0.28	$2f_{7/2}$	46
^{141}Ce	0.00	$2f_{7/2}$	33
	0.67	$3p_{3/2}$	168
	1.14	$3p_{1/2}$	104
	1.50	$2f_{5/2}$	2.6
	1.78	$2f_{5/2}$	2.1
	2.41	$(3p_{1/2})$ $(3p_{3/2})$	36 19
^{143}Nd	0.00	$2f_{7/2}$	49
	0.74	$3p_{3/2}$	250
	1.31	$3p_{1/2}$	165
	1.56	$2f_{5/2}$	5.08
	1.92	$2f_{5/2}$	1.68
^{145}Sm	0.00	$2f_{7/2}$	77
	0.89	$3p_{3/2}$	442
	1.61	$3p_{1/2}$	367

and only an average change of 0.04% in Λ_{lj} for the $f_{7/2}$, $p_{3/2}$, $p_{1/2}$, and $f_{5/2}$ state in ^{141}Ce .

These variations show that the reduced normalization is much less sensitive to the neutron pa-

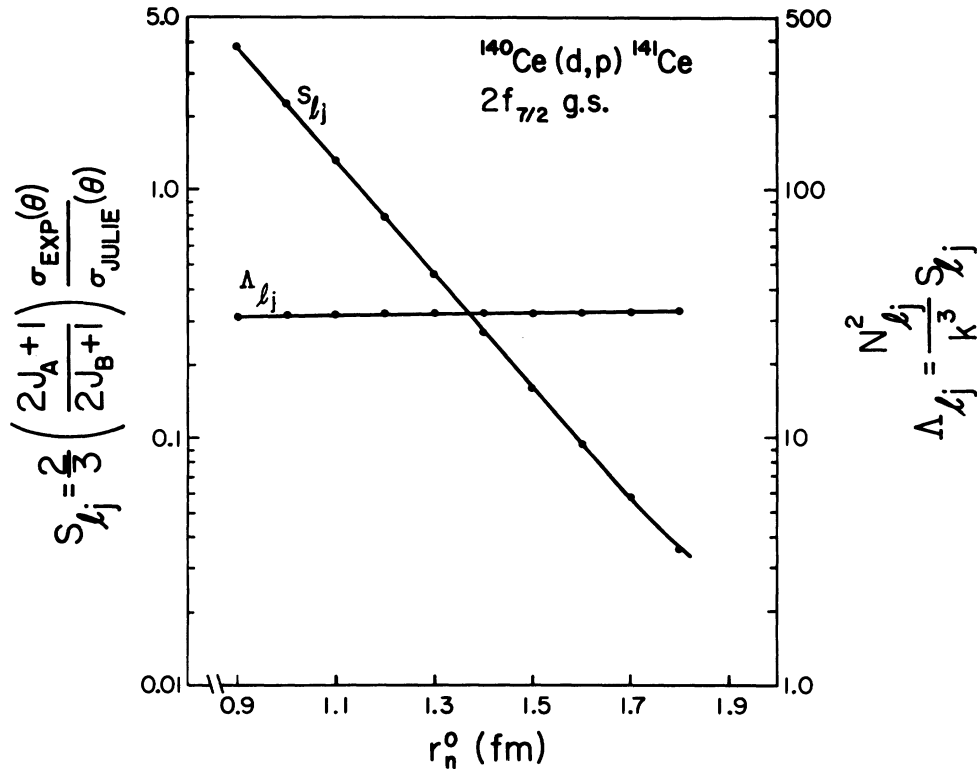


FIG. 6. Variation of the neutron well radius for the $^{140}\text{Ce}(d,p)$ g.s. reaction. r_n^0 was varied from 0.9 to 1.8 fm while all other parameters were held constant to the values shown in Table I. The solid line is used only to connect the points.

rameters than is the spectroscopic factor, as expected. When fitting (d, p) angular distribution data with DWBA calculations, this is a distinct advantage, since the neutron radius and diffusivity act as scale factors within a certain range; that is, they merely move the DWBA curve up or down, without changing its shape, making it difficult to arrive at a unique value for S_{ij} . We were able to vary r_n^0 between 0.9 and 2.25 fm without producing any change in the shape of the DWBA curve; however, the curve was shifted up in scale by a factor of 100.¹¹

The variation of deuteron and proton potential parameters in the DWBA analysis yields no new information as to the distinction between Λ_{ij} and S_{ij} since Λ_{ij} and S_{ij} differ only by the factor N^2/k^3 , which is dependent only on neutron parameters. It was noted, however, that the deuteron parameter variations produce less of a change in Λ_{ij} and S_{ij} than the proton potential parameters. This is expected since the deuteron channel averages approximately 3.5 MeV below the Coulomb barrier for a 5.8-MeV deuteron beam on the $N=82$ isotones, while the proton channel is only 0.4 to 1.0 MeV below the Coulomb barrier due to large positive Q values.

It was also noted, but not understood, that variations of the real potential in the proton channel produce a larger change in S_{ij} and Λ_{ij} for the ground state of ^{145}Sm than they do for S_{ij} and Λ_{ij} of the ground state of ^{141}Ce . However, variation of the surface absorption potential (W, a', r_0') in the proton channel produces a larger change in S_{ij} and Λ_{ij} for ^{141}Ce than for ^{145}Sm . The latter effect can be explained in that the Coulomb barrier for ^{141}Ce is lower than that of ^{145}Sm , allowing the nuclear potential to have a greater effect in the stripping process. However, this should also

be the case for V as well as W , which it is not.

In the deuteron potential the most sensitive parameter was r_0' , the radius parameter of the surface absorption potential. When r_0' was varied from 1.0 to 1.4 fm, Λ_{ij} increased by 35% for the ground state of ^{141}Ce . In the proton potential the most sensitive parameter was r_0 , the real potential well radius. When r_0 was varied from 1.0 to 1.4 fm, Λ_{ij} increased 31% for the ground state of ^{141}Ce and 41% for the ground state of ^{145}Sm .

IV. RESULTS

The uncertainties in the reduced normalization are due primarily to errors in the target thickness and the statistical uncertainties due to low proton yields. As stated in a previous section, the target thicknesses are known to within $\pm 10\%$, while the statistical uncertainties in the yields average approximately 8 to 12%. Therefore, errors in the reduced normalizations are estimated at $\pm 20\%$. Also, since the sub-Coulomb (d, p) angular distribution exhibits very little structure, spin assignments for the various states had to be taken from the available literature. The final values for Λ_{ij} are shown in Table II.

As stated earlier, the density of states in ^{140}La and ^{142}Pr was very great due to proton coupling to neutron states. However, it was possible to do some DWBA analysis for the $^{139}\text{La}(d, p)$ reaction. The first peak of interest in the ^{140}La spectra occurred at an excitation energy of 40 keV and contained six states, all of which are $2f_{7/2}$ neutron states coupled to either a $1g_{7/2}$ or $2d_{5/2}$ proton state.⁷ This peak was treated as a single neutron state. The second peak of interest was a single-state $2f_{7/2}$ neutron state coupled to the $1g_{7/2}$ proton state with $J=7$, at an excitation energy of 0.28 MeV. It should be noted, however, that these values of Λ_{ij} were calculated without taking into account the rather strong proton coupling.

In the ^{141}Ce spectra, a total of nine states was observed. For three of the states, $E_x=2.18, 2.32,$ and 2.52 MeV, the spins were not well known, and therefore the DWBA analysis could not be done. At an excitation energy of 2.41 MeV a fairly intense state was observed (P_7 in Fig. 1), as noted by Holms and Martin,¹² which is thought to be either $p_{1/2}$ or $p_{3/2}$. When the DWBA analysis was carried out on this state for each spin assumption, the scale of the DWBA curves and the shape of the curves remained approximately the same. For the remaining five states the spins are well known.¹²⁻¹⁷

In the ^{143}Nd spectra a total of eight states were observed. However, the states at 3.54 and 2.56 MeV could not be separated within the resolution

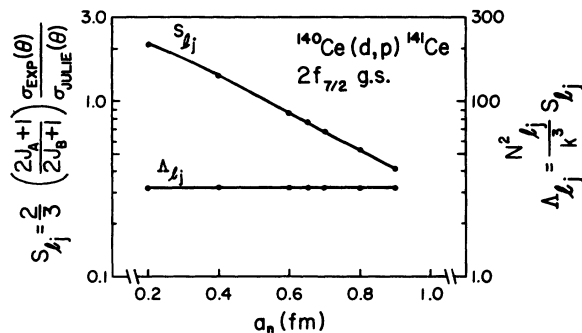


FIG. 7. Variation of the neutron well diffusivity for the $^{140}\text{Ce}(d, p)$ g.s. reaction. The diffusivity a_n was varied from 0.2 to 0.9 fm while all other parameters were held constant to the values shown in Table I. The solid line is used only to connect the points.

of our electronics, and the spin of the state at 1.86 MeV is not well known, therefore the DWBA analysis could not be done for these three levels. Note, in Fig. 3, that the state of 1.92 MeV was observed at only two angles. This was because of light contaminants moving through the peak of interest. However, since only one data point in the angular distribution is required to normalize the DWBA curve, the reduced normalization could be calculated. Thus, Λ_{ij} was obtained for five states, using spins found in the literature.^{13, 14, 17, 18}

Due to the high Coulomb barrier, the yields for the $^{144}\text{Sm}(d, p)$ reaction were very low, allowing only five states in ^{145}Sm to be separated from the background contaminants. The states at 1.98 and 2.00 MeV were too close to be separated with the resolution available in this experiment. Therefore, the DWBA analysis was done on only three states in ^{145}Sm . Fortunately, the spins of these states have been determined.^{13, 19-21}

V. DISCUSSION

Trends were noted in Λ_{ij} for different Q values and mass numbers. The (d, p) values for Λ_{ij} are shown in Figs. 8 and 9 for the $2f_{7/2}$ ground state. The natural log of Λ_{ij} appears to be approximately

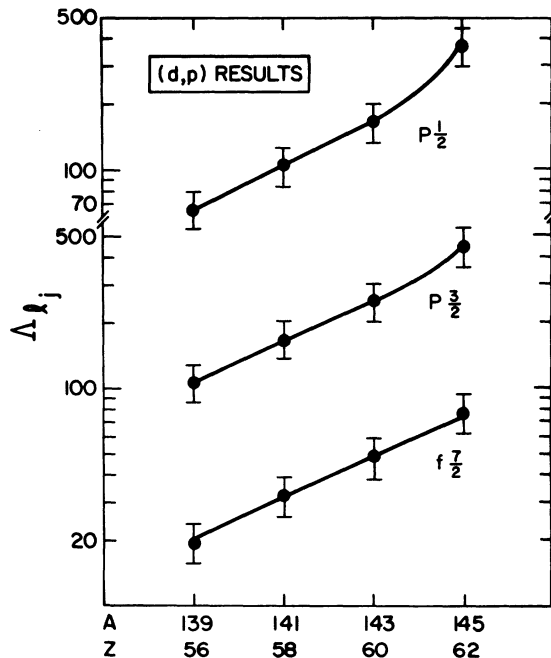


FIG. 8. The reduced normalization from sub-Coulomb stripping versus the mass number and charge number of the $N = 83$ isotones. The solid lines are only to guide the eye. The error bars represent the $\pm 20\%$ uncertainty in Λ_{ij} . For all three states, a straight line can be drawn through the four error bars.

proportional to the Q value and mass number. This also appears true for the $p_{3/2}$ first excited state; however, for the $p_{1/2}$ state, the ^{145}Sm reduced normalization has a higher value than would be expected by a Q value or mass-number proportionality.

This same dependence was also noted when the excitation energy was varied for the $3p_{3/2}$ state in ^{141}Ce , keeping the parameters in Table I constant. (The excitation energy of the $3p_{3/2}$ state is normally taken to be 0.67 MeV.) Values of the excitation energy were taken from 0.5 to 1.0 MeV, which is identical to varying the Q value from 2.71 to 2.21 MeV. When the natural log of Λ_{ij} and S_{ij} were plotted against the Q value a straight line resulted, with Λ_{ij} having the steeper slope. Λ_{ij} decreased from a value of 199.3 at an excitation energy of 0.5 MeV to 103.0 at an excitation energy of 1.0 MeV, a 48% drop. S_{ij} decreased from 0.48 to 0.34, a 24% drop. Thus, while Λ_{ij} is insensitive to the optical-model parameters, it is more sensitive to the excitation energy than is the spectroscopic factor.

From the definition of Λ_{ij} , the reduced normalization is dependent on three factors that involve the mass number and Q value; the wave number k , a spherical Hankel function $h_{ij}^{(w)}(ikr)$, and the transferred neutron's wave function $\langle B|A \rangle$. The A and Q dependence in k and $h_{ij}^{(w)}(ikr)$ is easily determined; however, this is not true for $\langle B|A \rangle$. $\langle B|A \rangle$ is determined by a Schrödinger equation which involves a Woods-Saxon potential and spin-

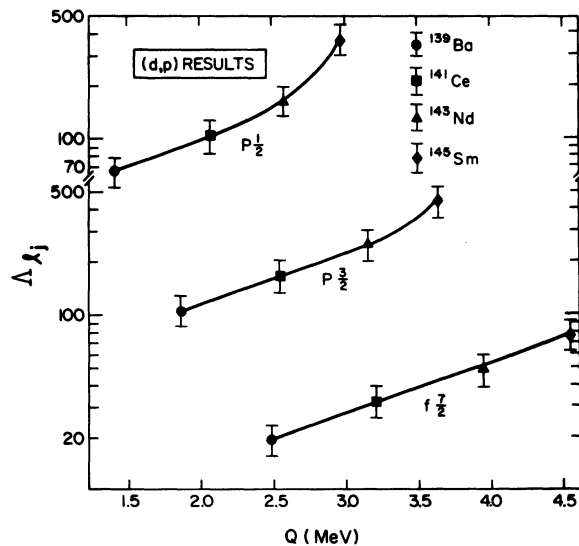


FIG. 9. The reduced normalization from sub-Coulomb stripping versus the Q value for the (d, p) reaction. The solid line is only to guide the eye. A straight line can be drawn through all the error bars for the $f_{7/2}$ and $p_{3/2}$ states.

orbit terms. Since this equation cannot be solved in closed form, the A and Q dependence of $\langle B|A \rangle$ is not easily determined, and therefore the dependence of Λ_{ij} on the mass number and Q value is not readily apparent.

VI. CONCLUSION

For several states populated in sub-Coulomb (d, p) reactions we have extracted a dimensionless quantity, the reduced normalization Λ_{ij} , which is independent of the optical-model parameter used in the DWBA analysis. It should be noted that the attractive feature of the reduced normalization's

parameter independence is somewhat offset by the fact that Λ_{ij} does not reflect the single-particle character of the neutron wave function as does S_{ij} .

Since this quantity Λ_{ij} can be extracted from isobaric-analog-resonance data,²² it is a valuable tool in comparing some of the available isobaric-analog-resonance theories to sub-Coulomb (d, p) results.^{9, 23, 24}

The authors would like to thank Dr. R. G. Seyler for his help in running code JULIE; also N. Tsoupas and Dr. J. W. Sinclair for their help with the data collection.

*Work supported in part by the National Science Foundation.

¹M. Dost and W. R. Hering, *Z. Naturforsch.* **21A**, 1015 (1966).

²P. J. A. Buttle and L. J. B. Goldfarb, *Nucl. Phys.* **78**, 409 (1966).

³J. Rapaport and A. K. Kerman, *Nucl. Phys.* **A119**, 641 (1968).

⁴R. H. Bassel, R. M. Drisko, and G. R. Satchler, Oak Ridge National Laboratory Report No. ORNL 3240, 1962 (unpublished).

⁵Micro Matter Company, 197-34th Ave. East, Seattle, Washington 98102.

⁶J. D. Goss, Ph. D. thesis, The Ohio State University, 1970 (unpublished).

⁷J. Kern, G. L. Struble, and R. K. Sheline, *Phys. Rev.* **153**, 1331 (1967).

⁸J. Kern, G. L. Struble, R. K. Sheline, H. R. Koch, B. P. K. Maier, U. Gruber, and O. W. B. Schult, *Phys. Rev.* **173**, 1133 (1968).

⁹J. F. Morgan, R. G. Seyler, and J. J. Kent, *Phys. Rev. C* **8**, 2397 (1973).

¹⁰J. Rapaport, A. Sperduto, and M. Salomaa, *Nucl. Phys.* **A197**, 337 (1972).

¹¹G. A. Norton, Ph. D. thesis, The Ohio State University, 1973 (unpublished).

¹²G. B. Holms and H. J. Martin, Jr., *Phys. Rev.* **122**, 1537 (1961).

¹³P. R. Christensen, B. Herskind, R. R. Borchers, and L. Westgaard, *Nucl. Phys.* **A102**, 481 (1967).

¹⁴C. A. Wiedner, A. Heusler, J. Solf, and J. P. Wurm, *Nucl. Phys.* **A103**, 433 (1967).

¹⁵W. Gelletly, J. A. Moragues, M. A. J. Mariscotti, and W. R. Kane, *Phys. Rev. C* **1**, 1052 (1970).

¹⁶F. W. Bingham and M. B. Sampson, *Phys. Rev.* **128**, 1796 (1962).

¹⁷R. H. Fulmer, A. L. McCarthy, and B. L. Cohen, *Phys. Rev.* **128**, 1302 (1962).

¹⁸C. L. Nealy and R. K. Sheline, *Phys. Rev.* **155**, 1314 (1967).

¹⁹R. K. Jolly and C. F. Moore, *Phys. Rev.* **145**, 918 (1966).

²⁰R. A. Kenefick and R. K. Sheline, *Phys. Rev.* **139**, B1479 (1965).

²¹E. Newman, K. S. Toth, and J. R. Williams, *Phys. Rev. C* **7**, 290 (1973).

²²R. G. Clarkson, P. von Brentano, and H. L. Harney, *Nucl. Phys.* **A161**, 49 (1971).

²³G. A. Norton, H. J. Hausman, and J. F. Morgan, following paper, *Phys. Rev. C* **9**, 1601 (1974).

²⁴G. A. Norton, H. J. Hausman, J. J. Kent, J. F. Morgan, and R. G. Seyler, *Phys. Rev. Lett.* **31**, 769 (1973).